JOURNAL OF CATALYSIS **166,** 347–355 (1997)
ARTICLE NO. CA971527

The Hydrogenation of *o*-, *m*-, and *p*-Xylene over Ni/SiO_2

Mark A. Keane

Department of Chemical Engineering, The University of Leeds, Leeds LS2 9JT, United Kingdom

Received July 31, 1996; revised November 4, 1996; accepted November 6, 1996

The gas phase hydrogenation of *o*-, *m*-, and *p*-xylene was studied over a Ni/SiO_2 catalyst prepared by homogeneous precipitation/deposition. The hydrogenation of each xylene yielded steroisomeric product mixtures of the saturated dimethylcyclohexane. The stereospecificity of the reaction is related to the nature of the reactant/catalyst interaction which governs the mode of addition of hydrogen to the carbons bearing the methyl substituents. The appearance of a common well-defined reversible maximum (T_{max}) in the rate vs. temperature plots is reported and discussed. Reaction orders with respect to xylene partial pressures are plotted as a function of reaction temperature. The temperature dependence of the rate constants was fitted to an Arrhenius equation and generated positive ($T \leq T_{max}$) and negative ($T \geq T_{max}$) activation energies. The derivation of true activation energies and heats of adsorption from the kinetic data is presented. Turnover frequencies at a particular temperature decreased in the order *p*-xylene > *m*-xylene > *o*-xylene. The respective roles of steric and electronic effects in determining the strength of adsorption and surface reactivity are discussed. A compensation effect, which is established for the experimentally determined or apparent kinetic parameters, is attributed to variations in the temperature dependencies of the surface concentration of the reactive species.

INTRODUCTION

The heterogeneous hydrogenation of aromatic compounds is normally carried out with platinum, rhodium, ruthenium, palladium, or nickel based catalysts, in many cases at elevated temperatures and/or pressures (1). In view of the stringent environmental regulations governing the aromatic level in diesel fuels, aromatic hydrogenation has become a key upgrading parameter in processing middle distillates (2). Taking an overview of the various compilations of the literature on this topic (1–8), it is readily apparent that benzene has been the overwhelming choice as the model aromatic feedstock. The rate of aromatic ring hydrogenation is however influenced by both steric and electronic factors (1–4). In general, hydrogenation rates decrease with ring substitution by alkyl groups unless the substituents introduce exceptional strain in which case the strained aromatic systems undergo facile saturation (3). The liquid (9–14) and gas (2, 15–22) phase hydrogenation of the xylenes over diverse catalyst systems have been reported. However, the xylene hydrogenation activity has, in the main, been presented as a percentage conversion or a rate relative to the rate of benzene hydrogenation. Rahaman and Vannice (22) have recently provided the first steady-state specific gas phase activities and activation energies for a series of unsupported and supported palladium catalysts. The results presented in this paper are a natural continuation of earlier investigations of benzene and toluene hydrogenation over supported nickel systems (23–26) and represent, to the best of the author's knowledge, the only steady-state kinetic study of *o*-, *m*-, and *p*-xylene hydrogenation on Ni/SiO_2. The objective of this report is to establish the role of structural isomerism in determining activity and selectivity in catalytic aromatic hydrogenation systems.

METHODS

The catalyst was prepared by the homogeneous precipitation/deposition of nickel onto a nonporous microspheroidal Cab–O–Sil 5M silica of surface area 194 $m^2\ g^{-1}$ as has been described in detail elsewhere (27). The catalyst precursor has a nickel loading of 1.5% w/w and low water content (<1% w/w). The hydrated catalyst precursor was reduced, without a precalcination step, by heating in a 150 $cm^3\ min^{-1}$ stream of dry hydrogen (99.9%) at a fixed rate of 5 K min^{-1} to a final temperature of 723 ± 1 K which was maintained for 18 h. Temperature-programmed reduction studies revealed a complete reduction of the nickel content to Ni^0 (28). The nickel metal dispersion, reproducible to better than $\pm 3\%$, expressed as $(Ni_{surface}/Ni_{total}) \times 100\%$ equals 73%. The supported nickel particle size is estimated to be 1.4 nm from the relationship (29) $d = 101/D$, where D is the dispersion and d represents the surface weighted average crystallite diameter assuming (spherical) particles ≤ 1 nm to be 100% dispersed. A value of 0.633 nm^2 for the average surface nickel atom (30) yields a surface area of 74 $m^2\ g^{-1}$. Repeated use of the catalyst did not result in any change in the dispersion or dimensions of the supported nickel crystallites.

All the catalytic reactions were carried out under atmospheric pressure in a fixed-bed glass reactor over the

0021-9517/97 $25.00

temperature range 393 K $\leq T \leq$ 523 K. Details of the catalytic reactor, procedure, and analysis are available elsewhere (23). All the activity data presented in this paper were obtained at steady state and are the average of at least six separate test samples. The kinetic measurements were made using catalyst meshed in the 125–150 μm range at a space velocity of 2×10^3 h^{-1} (STP) and in the *W/F* range 42–112 g mol^{-1} h, where *W* is the weight of activated catalyst and *F* is the flow rate of aromatic. Mol% conversion was kept below 20% by varying *W* in order to minimize heat and transfer effects. The reactor has been shown previously (23) to operate in the absence of appreciable diffusion limitations under the stated experimental conditions. The reaction order with respect to the three aromatics was measured at a constant hydrogen pressure of 0.94 atm, where the pressure of each aromatic was varied in the range 0.01–0.06 atm, using nitrogen as the makeup gas. Molar selectivity in terms of product *x* is defined as $m_x/m_{\text{tot}} \times 100$, where m_{tot} is the total number of moles of product. The *o*-, *m*-, and *p*-xylene (Aldrich, 98+%) reactants were thoroughly degassed by purging with purified helium and were stored over activated molecular seive type 5 A.

RESULTS AND DISCUSSION

The hydrogenation of *o*-, *m*-, and *p*-xylene over Ni/SiO_2 yielded 1,2-, 1,3-, and 1,4-dimethylcyclohexane (DMC), respectively, as the only hydrogenated products. The saturated cylcloparaffin products were present as a mixture of the *cis* and *trans* forms. An isomerization of *o*-xylene to *m*-xylene, which has been reported for palladium systems (22), or a partial hydrogenation to dimethylcyclohexenes, as has been observed for liquid phase reactions (9, 11), was not detected in this study. Passage of each aromatic in a stream of hydrogen over the silica support did not result in any measurable degree of hydrogenation. At temperatures in excess of 523 K each xylene feed was observed to undergo partial hydrogenolysis with the result that this investigation has been limited to temperatures ≤523 K. The effect of temperature on the turnover frequency (TOF) or the number of xylene molecules converted per metal site per second is illustrated in Fig. 1. The only available steady state TOFs in the literature refer to palladium systems at 413 K (22) and these are 1.3–59 times greater the values generated in this study. It is however well established that the aromatic ring hydrogenation activity of palladium is greater than that of nickel (3, 31). The addition of methyl group(s) to the aromatic ring has been found to lower the rate of ring hydrogenation and the ease of reduction has been shown (3, 4, 13, 22) to decrease in the order benzene > toluene > xylene. The TOFs of the three xylenes recorded in this study are very close but do increase in the order *o*-xylene < *m*-xylene < *p*-xylene, over the entire temperature range that was studied. Rahaman and Vannice

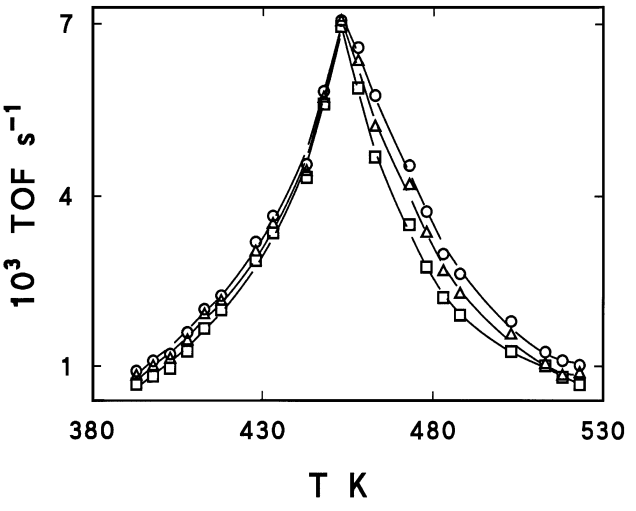

FIG. 1. The temperature dependence of the turnover frequency of *o*-xylene (□), *m*-xylene, (△) and *p*-xylene (○).

(22) noted that the rate of hydrogenation of *o*-xylene over palladium was four to six times lower than that of *m*-xylene and the latter hydrogenated at comparable or slightly lower rates than *p*-xylene. The relative TOF for *o*-: *m*-: *p*-xylene at representative temperatures are given in Table 1. While the relative specific rates vary appreciably with temperature, the differential observed between the three xylenes is not as great as that reported for palladium (22). Benzene is known to be adsorbed on nickel via π-bond interactions and it is now generally accepted that the presence of methyl substituents on the benzene ring stabilizes the adsorbed π-complex with the resultant introduction of a higher energy barrier for aromatic ring hydrogenation (32–34). From a consideration of the observed sequence of activities, it may be concluded that the adsorbed *o*-xylene π-complex is the most stable or least reactive of the three xylenes. It has been proposed that the stability of π-complexes increases with decreasing ionization potential (21). However, the ionization potential (35) of *p*-xylene (8.44 eV) is lower

TABLE 1

The Temperature Dependence of the Relative Turnover Frequencies of the Three Xylenes

T (K)	Relative TOF *o*-Xylene : *m*-Xylene : *p*-Xylene
393	1 : 1.19 : 1.34
408	1 : 1.14 : 1.26
428	1 : 1.05 : 1.12
443	1 : 1.02 : 1.05
458	1 : 1.08 : 1.12
473	1 : 1.22 : 1.33
488	1 : 1.23 : 1.33
503	1 : 1.24 : 1.36
518	1 : 1.30 : 1.49

than that of *o*- (8.56 eV) and *m*- (8.58 eV) xylene which are essentially the same. The differences in activity exhibited by the three xylenes is not due, therefore, primarily to an electronic effect. An alternative explanation which invokes the contribution of steric constraints due to the neighboring methyl groups will be supported by subsequent kinetic data. A feature of the three plots shown in Fig. 1 is the presence of a common temperature related activity maximum (T_{max}) at 453 K. The source of such a maximum may be arrived at by considering the obvious causes. Each maximum could be traversed from either the high or low temperature side without any loss in activity which, in effect, negates catalyst deactivation as a possible cause. Diffusion effects can be discounted as the catalytic reactor is known (23) to operate in the differential mode and the degree of hydrogenation was far from equilibrium conversions. Nickel crystallite growth during catalysis can, likewise, be excluded. The possible contribution of the reverse, dehydrogenation, reaction to the observed maxima in hydrogenation rates was investigated by passing each of the saturated cycloparaffins over the activated catalyst. There was no measurable dehydrogenation of the cycloparaffin feed at $T \leq 473$ K. The existence of a temperature dependent benzene (24) and toluene (25) hydrogenation maximum has been ascribed in the case of Ni/Y zeolites to a decrease in the surface coverage by the aromatic with increasing temperature which at some point results in a decrease in the reaction probability. In the absence of catalyst deactivation, secondary reactions, changes in active site distribution, product inhibition and thermodynamic and diffusion effects, it is reasonable to also attribute the occurrence of the common T_{max} for the conversion the three xylenes over Ni/SiO_2 to adsorption phenomena.

The kinetics of the reaction may be represented by the power equation

$$\mathrm{TOF} = k P_x^m P_{H_2}^n, \qquad [1]$$

where k is the rate constant, P_x and P_{H_2} the partial pressure of the particular xylene reactant and hydrogen and m and n the orders of the reaction with respect to the aromatic and hydrogen partial pressures, respectively. The reaction orders with respect to xylene were determined by means of logarithmic plots where at constant reaction temperature and P_{H_2}

$$\log \mathrm{TOF} = \log\left(k P_{H_2}^n\right) + m \log P_x. \qquad [2]$$

and plots of log TOF against $\log P_x$ yield m. The orders with respect to xylene partial pressure derived from the experimental data are plotted as a function of temperature in Fig. 2. Representative logarithmic plots depicting the variation of TOF with the partial pressure of *m*-xylene at selected temperatures are shown in the inset to Fig. 2. The value of m increased from <0.1 to 0.44 as the temperature was raised from 393 to 523 K. The author could find no documented temperature dependence of reaction orders in xylene hydrogenation reactions on comparable nickel/amorphous carrier systems. The near zero order

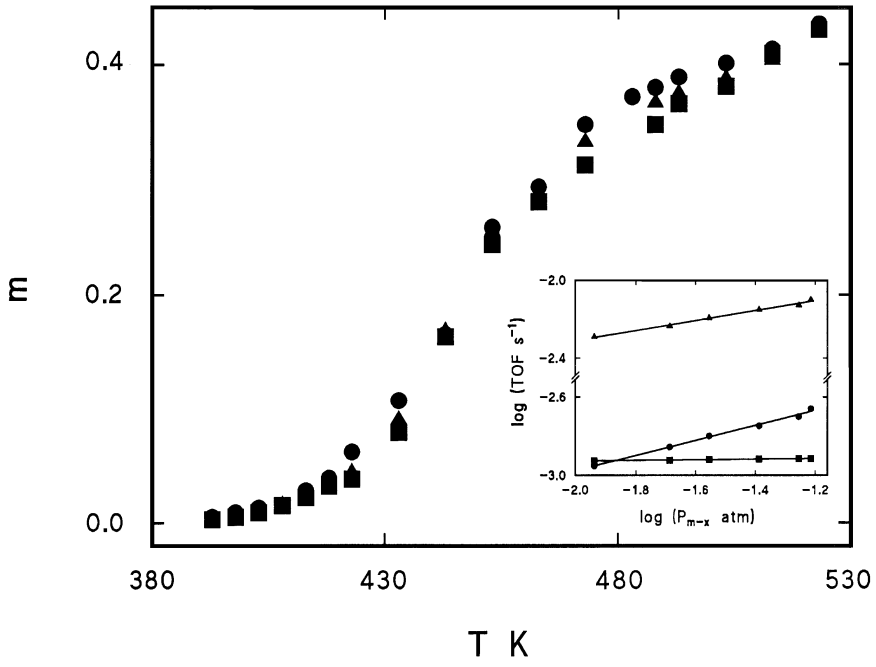

FIG. 2. Dependence of the reaction order (m) with respect to the partial pressure of *o*-xylene (■), *m*-xylene (▲), and *p*-xylene (●). (Inset) TOF of *m*-xylene as a function of partial pressure at 403 K (■), 453 K (▲), and 503 K (●).

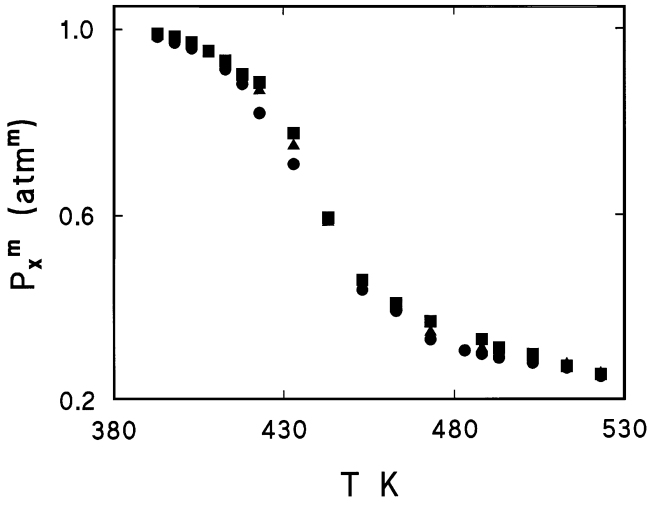

FIG. 3. Variation with temperature of P_x^m, where x represents *o*-xylene (■), *m*-xylene (▲), and *p*-xylene (●): $P_x = 0.04$ atm.

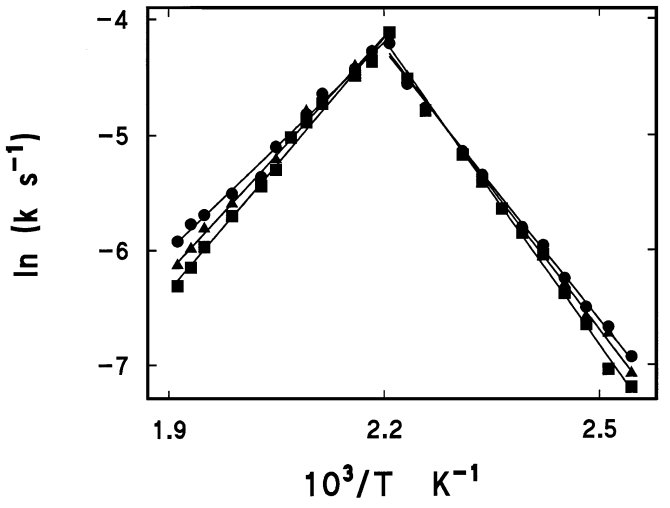

FIG. 4. Apparent Arrhenius plots for the hydrogenation of *o*-xylene (■), *m*-xylene (▲), and *p*-xylene (●).

dependence on all three aromatics observed in this study where $m < 0.1$ at $T \leq 433$ K is consistent with a high surface coverage by the aromatic. The increase in the reaction order with increasing temperature suggests that the surface coverage is lower at higher temperatures. The values of m are very close for the three xylene reactants but the experimental values at a particular temperature do exhibit a definite increase in magnitude (where $T > 430$ K), in the order *o*-xylene < *m*-xylene < *p*-xylene. In a bimolecular surface reaction, the reaction rate is proportional to the surface coverage (θ) of both reactants, i.e.,

$$\text{TOF} = k\theta_x\,\theta_{H_2}. \qquad [3]$$

From Eqs. [1] and [3] it follows that $\theta_x \propto P_x^m$ and the variation of the surface coverage by the xylene reactants may be approximated by the temperature dependence of the experimentally determined P_x^m values and these relationships are plotted in Fig. 3. The influence of increasing temperature on P_x^m and by inference on the fractional surface coverage is considerable. Under the stated experimental conditions, the reaction order with respect to the hydrogen concentration (n) increased with temperature from 0.7 to 2.3. However, the values of $P_{H_2}^n$ have been shown to be largely unaffected by temperature and to be independent of the nature of the aromatic (23), an observation which is taken to be indicative of a noncompetitive adsorption of the reactants during catalysis. The temperature dependence of TOF shown in Fig. 1 can then be considered to essentially mirror the combined effect of an increase in the rate of hydrogenation on the catalyst surface and the accompanying decrease in the concentration of surface reactive aromatic species which ultimately results in the generation of a T_{max}.

The rate constants (k, units of s^{-1}) for the three reactions were calculated using Eq. [1] and the experimental Arrhenius relationships are shown in Fig. 4. The computed activation energies (with 95% confidence limits) and the associated temperature independent preexponential factor (A), often referred to as the reaction frequency factor, are given in Table 2 where

$$k = A_{app}\exp(-E_{app}/RT). \qquad [4]$$

The activation energy values for the three xylenes are very similar and there is some overlap within the 95% confidence band. Nevertheless, at $T \leq 453$ K, there is a discernible trend of increasing values in going from the *p*- to *m*- to *o*- forms which agrees with the observed sequence of TOFs. Steady-state activation energies (31–82 kJ mol^{-1}) generated from a range of palladium catalysts (22) encompass the values reported in this paper, while the values quoted for *o*- and *p*-xylene reduction (39–59 kJ mol^{-1}) over Pt, Pd, and Pt/Pd supported (on alumina) systems using a pulse reactor (18) are appreciably lower. The temperature dependence of the rate constants at $T \geq T_{max}$ also obey the Arrhenius relationship and yield the negative activation energies which are

TABLE 2

Kinetic Data Obtained from the Arrhenius Relationships Shown in Fig. 4

Xylene feed	T range (K)	A_{app} (s^{-1})	E_{app}[a] (kJ mol^{-1})
o-Xylene	393–453	4×10^6	73.4 ± 3.8
	453–523	2×10^{-9}	-60.5 ± 3.0
m-Xylene	393-453	1×10^6	68.1 ± 3.4
	453–523	6×10^{-9}	-56.1 ± 3.3
p-Xylene	393–453	4×10^5	64.9 ± 2.6
	453–523	3×10^{-8}	-49.6 ± 3.2

[a] With 95% confidence limits.

included in Table 2. In heterogeneously catalyzed systems, the activation energies obtained from the relationship between the experimentally obtained rate constants and temperature are generally accepted to be apparent activation energies as the surface coverage by the reactive species does not remain constant throughout the temperature range studied. Consequently, apparent values of $A(A_{app})$ and $E(E_{app})$ are obtained by application of the Arrhenius equation to the overall rate data and these parameters do not directly refer to the rate-limiting surface bond redistribution step. The true activation energy (E_{true}) is obtained by adding the enthalpy of adsorption as a positive quantity to the apparent activation energy (36, 37)

$$E_{true} = E_{app} - \Delta H_{ads}. \quad [5]$$

The process of chemisorption also has an activation energy (E_{ads})

$$k_{ads} = \sigma Z \exp(-E_{ads}/RT), \quad [6]$$

where k_{ads} is the rate coefficient for chemisorption, σ is the sticking probability or fraction of collisions that leads to adsorption, and Z is the number of collisions per unit area per unit time. This equation, based on collision theory, is analogous to Eq. [4]. Desorption is an activated process since the minimum E_{des} is that equal to ΔH_{ads}, where (12, 38, 39)

$$E_{des} - E_{ads} = \Delta H_{ads}. \quad [7]$$

Each of the xylene hydrogenations reported in this study where conducted in the absence of (a) diffusion/mass transport effects, (b) rate inhibition by the products, and (c) secondary reactions and, as such, may be considered to be surface controlled where the overall reaction rate is governed by the surface concentration of the reactive species. The activation energies obtained over the temperature ranges corresponding to increasing and decreasing rate constants are, therefore, essentially equivalent to E_{ads} and E_{des}, respectively. Taking each set of experimentally evaluated activation energies, values of ΔH_{ads} and E_{true} for the three cases were obtained from a combination of Eqs. [5] and [7] and are quoted with 95% confidence limits in Table 3. The order of increasing E_{true} is the same as that of E_{app} and there is a definite increase in ΔH_{ads} values in going from *p*- to *m*- to *o*- substitution. The author could find no spectroscopic study of *o*-xylene adsorption on metals. Nevertheless, the strength of xylene adsorption has been considered to be greater than that of benzene as a result of the stronger donation from the π-electron cloud to the metal due to the presence of the methyl groups (40, 41); i.e., the effect is electronic in nature. Differences in ΔH_{ads} within the family of xylenes can however result from steric effects. Minot and Gallezot, in a theoretical investigation (29), found that toluene adsorbs parallel to the active surface and the C–H and C–CH_3 bonds bend away from the surface. In the case of xylene adsorption both methyl groups must be bent away from the surface in order to relieve the steric repulsion. The repulsive potential is greatest in the case of neighbouring or *ortho*-methyl groups with the result that *o*-xylene has to overcome the largest barrier and the adsorption energy must be greatest as is the case with the inferred values given in Table 3. The aromatic ring distortion which allows the methyl substituents to point away from the plane of the ring must then increase in going from *p*- to *m*- to *o*-xylene. An increase in the energy of interaction with the surface is accompanied by a decrease in reactivity with the consequent sequence of TOFs shown in Fig. 1 and Table 1.

TABLE 3

Values of E_{app}, ΔH_{ads}, and E_{true} with 95% Confidence Limits Obtained from the Arrhenius Relationships shown in Fig. 4

Xylene feed	E_{app} (kJ mol^{-1})	ΔH_{ads} (kJ mol^{-1})	E_{true} (kJ mol^{-1})
o-Xylene	73.4 ± 3.8	-133.9 ± 4.8	207.3 ± 6.1
m-Xylene	68.1 ± 3.4	-124.2 ± 4.7	192.3 ± 5.7
p-Xylene	64.9 ± 2.6	-114.5 ± 4.1	179.4 ± 4.7

It is often observed (12, 42, 43), in the case of either the same reaction conducted over a series of different catalysts or a series of related reactions conducted over the same catalyst, that a relationship exists between E_{app} and A_{app} which takes the form

$$\ln A_{app} = eE_{app} + B. \quad [8]$$

The above relationship is termed the compensation effect (CE), where e and B are compensation factors. The effect is aptly named as an increase in $\ln A_{app}$ is offset or compensated by an increase in E which results in a decrease in reaction rate. The preexponential factors (A_{app}) obtained in this study are plotted against the corresponding apparent activation energies in Fig. 5. It can be seen that the linear relationship (correlation coefficient >0.999) holds true for the three sets of positive and negative activation energies where $e = 0.264 \pm 0.007$ and $B = -4.199 \pm 0.046$. Previously reported data for the hydrogenation of benzene (24) and toluene (25) over Ni/K–Y and benzene and toluene over Ni/SiO_2 (23) are also included in Fig. 5 and are likewise consistent with Eq. [8]. A true compensation effect is established if a single point of concurrence appears in the Arrhenius plots (12, 42, 45). The temperature corresponding to such a point, the isokinetic temperature (T_{iso}) is obtained from

$$T_{iso} = \frac{1}{eR}, \quad [9]$$

where e is the slope of the compensation plot and R is the gas constant; the calculated value of T_{iso} is 456 ± 8 K. The experimentally determined rate constants at 453 K

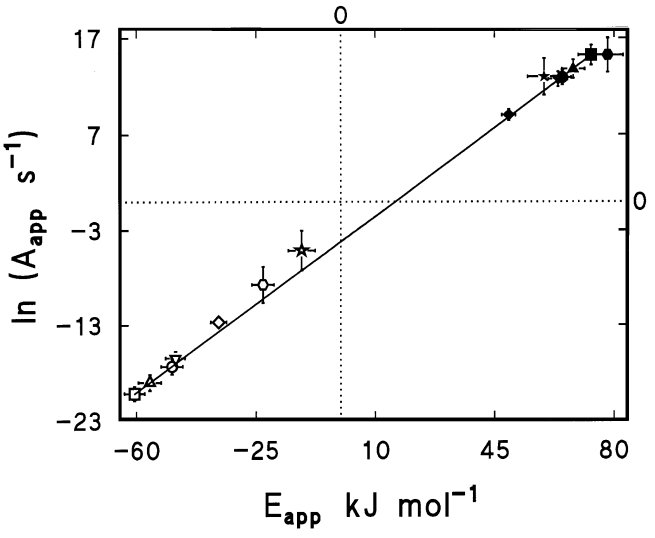

FIG. 5. Compensation plot for the hydrogenation of *o*-xylene (■, □), *m*-xylene (▲, △) and *p*-xylene (●, ○) over Ni/SiO_2 where the equation of the fitted line is $\ln A_{app} = (0.264 \pm 0.007)E_{app} - 4.199 \pm 0.046$. Note: $\ln A_{app}$ vs. E_{app} data for the hydrogenation of benzene (◆, ◇) and toluene (▼, ▽) over Ni/SiO_2 (23) and the hydrogenation of benzene (★, ☆) (24) and toluene (⬣, ⬡) (25) over Ni/K–Y.

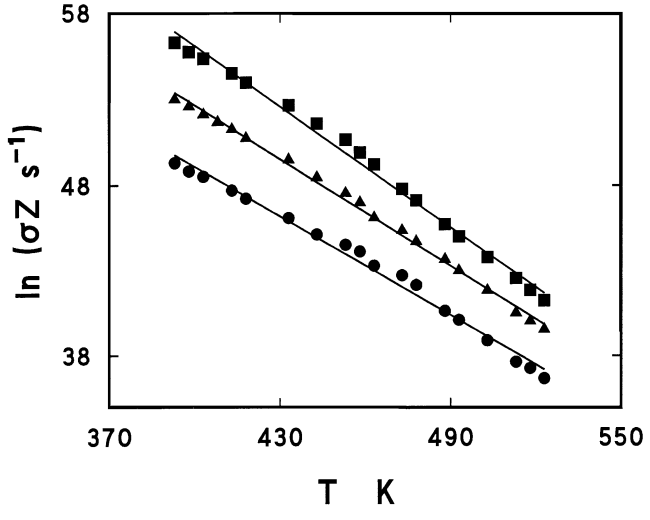

FIG. 6. The temperature dependence of $\ln \sigma Z$ for the hydrogenation of *o*-xylene (■), *m*-xylene (▲), and *p*-xylene (●).

yield the ratios $k_{o\text{-xylene}} : k_{m\text{-xylene}} : k_{p\text{-xylene}} = 1 : 1.01 : 1.02$. The agreement between the calculated and experimental T_{iso} values is good and confirms the attribution of a compensation effect to the hydrogenation of the three xylenes over Ni/SiO_2. The actual source of the compensation effect is still a matter of some debate and the validity of the effect as a kinetic observation and not merely an experimental artifact remains open to question. The kinetic investigation which yielded this compensation effect was conducted under experimental conditions where the enthalpy of the adsorption term is important; i.e., the CE is only obeyed by the experimentally determined or apparent A or E values. The true preexponential factor, corresponding to the true activation energy, must take account of both the probability of collision between the two reactants and the change in the surface concentration with temperature. A modified Arrhenius equation, based on collision theory

$$k = \sigma Z \exp(-E_{true}/RT) \qquad [10]$$

describes the true temperature dependence of the rate constant, where E_{true} refers to the rate determining step and the term σZ makes due allowance for variations with temperature in the probability of surface collisions. Values of σZ were calculated for each temperature using Eq. [10] and the relationship between σZ and T is illustrated in Fig. 6. The decrease in collision probability with temperature, depicted in the three plots, is diagnostic of a decreasing concentration of xylene on the catalyst surface. A plot of $\ln(k/\sigma Z)$ versus $1/T$ gives a slope of $-E_{true}/R$ according to Eq. [10] and the three plots generated using calculated values of E_{true} are shown in Fig. 7. Such plots illustrate the dependence on temperature of the rate constant for the true surface reaction and unlike the apparent Arrhenius relationships do not possess a single point of concurrence. It may be concluded that the compensation effect is a direct result of apparent kinetic measurements which yield composite kinetic parameters.

The hydrogenation of each xylene yielded stereoisomeric mixtures where the ratio of isomers in the product was constant at a particular temperature over the range of aromatic concentrations that were studied. The variation, with temperature, of the rate constant for hydrogenation to both *cis* and *trans* products is illustrated in Fig. 8 and the selectivity in terms of *trans* formation at representative temperatures

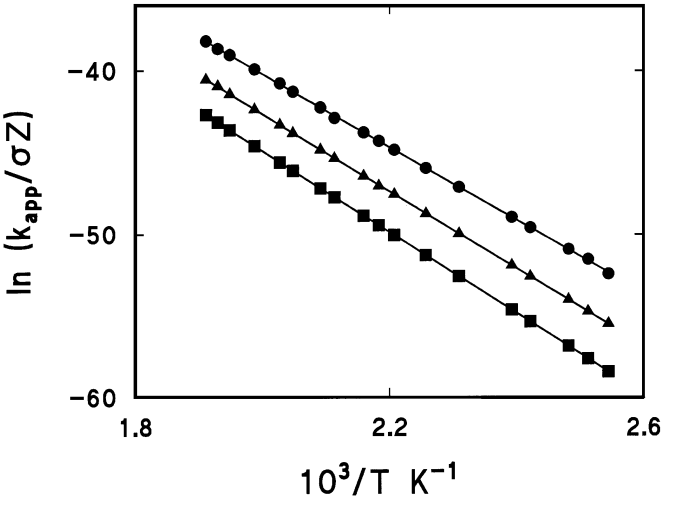

FIG. 7. True Arrhenius plots for the hydrogenation of *o*-xylene (■), *m*-xylene (▲), and *p*-xylene (●).

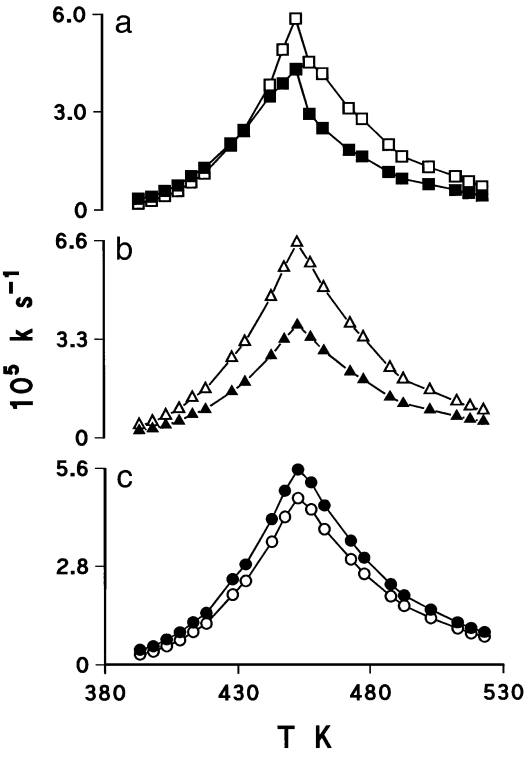

FIG. 8. The effect of temperature on the rate constant for the formation of the *trans* (open symbols) and *cis* (closed symbols) saturated product from (a) *o*-xylene (■, □), (b) *m*-xylene (▲, △), and (c) *p*-xylene (●, ○).

is recorded in Table 4. Practical interest in such selective hydrogenations is limited but the reactions may be considered as the simplest models to probe the effects of reaction variables on the stereochemistry of substituted aromatic reduction. The majority of the available literature (6, 9, 12, 14) in which the relative *cis/trans* product ratios are documented have dealt with reactions conducted in the liquid phase and the available selectivity data for gas phase hydrogenation (17–19) are scant. The principal product of the hydrogenation of dialkylbenzenes has largely been the *cis*-dialkylcyclohexane (6, 17, 18, 46, 47). An increase in the proportion of *trans* product from 1,2- and 1,4-dialkylbenzene with increasing temperature has been recorded (6, 12, 14). Hydrogen pressure and the size of the alkyl substituent have also been identified as factors which influence product distribution (9). In addition, the nature of the catalyst has been recognized as having a bearing on the stereoselective process (46). In this study, the hydrogenation of *o*-xylene preferably yielded *cis*- 1,2-DMC at $T < 428$ K, while the proportion of the *trans* product increased at higher temperatures to a maximum selectivity of ca. 63% which was essentially constant at $463\ \text{K} \leq T \leq 523$ K. In contrast, *m*-xylene was preferentially hydrogenated to *trans*-1,3-DMC at a percentage selectivity (ca. 63%) which was constant over the entire remperature range that was studied. The reduction of *p*-xylene produced a higher concentration of *cis*-1,4-DMC but the fraction of *trans*-1,4-DMC increased slightly with increasing temperature to give virtually equimolar mixtures at $T > 433$ K. Each pair of *cis/trans* 1,2-, 1,3-, and 1,4-DMC diastereomers exist in two interconvertible chair conformations. In the case of the 1,2- and 1,4- derivatives, the *trans* conformation is the more stable, whereas with the 1,3- derivative the reverse is true (48). The product distribution generated over Ni/SiO_2 clearly departs from the stereochemical equilibria. The observed selectivities, in turn, differ to a greater degree from the reported liquid phase data but direct comparisons are not very meaningful. The source of steroisomeric differentiation in a continuous flow gas phase system may well differ from that which controls stereoselectivity in a batch liquid phase process. While the interaction between substrate and catalyst has been proposed (9, 14) as the major factor that determines stereospecificity in the liquid phase, desorption of the diene has been shown to occur (9) and this intermediate can undergo a second hydrogenation step which may involve a different substrate/catalyst interaction. The liquid phase reaction is conducted in an organic medium that may also influence the stereospecific step. In the gas phase hydrogenation of the xylenes the stereochemistry of reduction must be determined at the adsorption step and the nature of the steric interaction between the reactant(s) and the catalyst surface determines the ultimate isomeric form of the saturated product. The gas phase hydrogenation of benzene has been viewed in the literature as occurring via the sequential addition of hydrogen atoms to the adsorbed aromatic where no rate determining step is apparent (49, 50) or where the addition of the first (51, 52), the second (22) or the sixth (51) hydrogen atom is the slow step. As the same compensation plot can be applied to benzene and methylbenzene hydrogenation (Fig. 5), the transformation of each aromatic may be tacitly assumed to proceed via the same rate demanding step. The destabilization of the resonance energy that is initiated by the addition of the first hydrogen

TABLE 4

The Effect of Temperature on the Selectivity to *trans* Dimethylcyclohexane formation for the Three Xylenes

	S_{trans} (%)		
T (K)	*o*-Xylene	*m*-Xylene	*p*-Xylene
393	40.3	63.3	41.0
408	43.7	63.3	42.9
428	49.2	63.4	45.1
443	52.4	63.2	45.8
458	59.5	63.4	45.9
473	62.9	63.4	45.9
488	63.5	63.4	46.0
503	63.2	63.3	45.9
518	63.6	63.3	46.1

should be very energetically demanding and is proposed to be the slow step. The observed increase in activation energy with increasing resonance energy of the aromatic nucleus is consistent with such a mechanism. The turnover frequency is influenced by the concentration of the surface reactive aromatic (23) and once equilibrium adsorption has been attained the rate of the overall surface reaction is governed by the rate of the slow step; the nature of this step is not controlled by adsorption phenomena. The true Arrhenius plots shown in Fig. 7 illustrate the temperature dependence of the surface reaction given in Eq. [3]. The direction of addition of hydrogen to the two carbons which bear the methyl group is controlled by the geometry of adsorbed moiety. It is assumed that the xylenes adsorb with the aromatic ring parallel to the surface and both methyl groups directed away from the surface in order to relieve the steric repulsion. At the lowest reaction temperature, *o*-xylene is preferably hydrogenated to *cis*-1,2-DMC which is the thermodynamically less stable of the two possible stereoisomers. Under these reaction conditions *o*-xylene is most strongly held at the surface and the crowding effects due to neighboring adsorbed molecules constrain the motion of each adsorbed species. In such a constrained system one of the hydrogen atoms that is added to a carbon which is bonded to a methyl group lies in the plane of the ring, while the other lies axially to the ring and one of the methyl groups is now oriented equatorially, the other axially. The adsorbed molecule therefore adopts a conformation which differs from the conformation of lowest energy in the isolated molecule. From adsorption studies of benzene and toluene and their saturated analogues (39, 53), it can be assumed that 1,2-DMC is not as strongly held on the surface as *o*-xylene and desorbs rapidly in the hydrogen gas stream in the stereoisomeric form that is generated as a result of the surface interactions. The more stable *trans* isomer is also produced at a comparable rate and is isolated as the principal product at $T > 433$ K. An increase in reaction temperature is accompanied by a decrease in the surface concentration of the active aromatic (as may be inferred from Fig. 6) and the geometrical constraints are somewhat relieved. It is proposed that the weakening of the surface interaction and decreased crowding with increasing temperature allows the rearrangement of atoms not directly involved in the binding process with a consequent increase in the proportion of *trans* product where both methyl groups are equatorial to the plane of the ring and van der Waals strain is reduced. Such a switch in stereoselectivity could also be due to a metal catalyzed epimerization or conformational inversion of one asymmetric carbon atom (14, 54, 55). Known mixtures of *trans/cis* 1,2-DMC (molar ratios in the range 0.17–0.58) were passed, in a stream of hydrogen, using the same experimental conditions as employed in hydrogenation step through an empty reactor, over the silica support and over activated Ni/SiO_2 at 393 K $\leq T \leq$ 523 K. The *trans/cis* ratios in the product mixtures were $\leq$1.2 greater than in the actual saturated feedstock which is considerably lower than the increase by a factor of 2.6 induced by temperature variations in the direct hydrogenation of *o*-xylene. Catalytic epimerization may be discounted as a principal contributory factor in determining stereodifferentiation in this particular study. The hydrogenation of *m*-xylene generated *trans*-1,3-DMC, the thermodynamically less stable stereoisomer, as the favored product which in common with *cis*-1,2-DMC, the initially preferred product from *o*-xylene, has one methyl group equatorially and one axially oriented with respect to the plane of the ring. However, the ratio of *cis/trans*-1,3-DMC is independent of temperature, as shown in Table 4, which suggests that a decrease in surface constraints did not result in a rearrangement of the adsorbed species to the more stable conformation. The *cis* isomer of 1,3-DMC is 7.5 kJ mol^{-1} more stable than the *trans* form compared with the 11.3 kJ mol^{-1} differential between *trans* and *cis* 1,2-DMC (47). It is therefore proposed that in the stepwise addition of hydrogen to *m*-xylene the possible reduction of van der Waals strain is not great enough to induce geometrical rearrangement of the adsorbed species as the reaction temperature is increased. In the case of *p*-xylene, steric hindrance in the mode of adsorption is not as severe with the result that the product mixture approaches equimolarity. Nevertheless, the *cis* product is preferred where, once again, one hydrogen is added axially and one equatorially to the carbons bearing the methyl groups. An increase in temperature favours, albeit marginally, the more stable *trans* isomer but as with 1,3-DMC the difference in energy (7.5 kJ mol^{-1}) between the two isomeric forms does not appear to be sufficient to result in an appreciable temperature effect.

CONCLUSIONS

The TOFs of the three xylenes increase, at steady state in the absence of diffusion constraints, catalyst deactivation and secondary conversions, in the order *o*-xylene < *m*-xylene < *p*-xylene in the temperature range 393 K $\leq T \leq$ 523 K. The specific rate of hydrogenation of each xylene passes through a maximum at a common temperature T_{max} (453 K) and this is attributed to a critical loss of the reactive aromatic species from the surface. The reaction order with respect to each xylene isomer increases with temperature from 0 to 0.44 where the value of the partial pressures raised to the particular reaction order is considered to reflect the changes in the fractional surface coverage. The variation of rate constant with temperature yields both positive and negative activation energies. Taking the reaction energies to be equivalent to the chemisorption energies, values of E_{true} and ΔH_{ads} can be evaluated where both parameters increase in the order *p*-xylene < *m*-xylene < *o*-xylene. Assuming the xylenes adsorb with the aromatic ring parallel

to and both methyl groups directed away from the surface, the repulsive potential is greatest in the case of neighboring or *o*-methyl groups with the result that the consequent adsorption energy is greatest. Hydrogenation yields stereoisomeric product mixtures where, due to steric constraints, one hydrogen is added axially and one equatorially to the two carbons bearing a methyl group. The above orientation is favored over the entire temperature interval for the hydrogenation of *m*- and *p*-xylene, whereas at $T > 433$ K, in the case of *o*-xylene the atoms not directly involved in the binding process are rearranged to relieve the van der Waal's strain and preferably generate the more stable *trans* isomer. A compensation effect has been observed for the relationship between $\ln A_{app}$ and E_{app} with a $T_{iso} = 456 \pm 8$ K and it is concluded that A_{app} and E_{app} are composite terms which incorporate contributions due to the temperature dependence of the surface concentration of the reactive species.

REFERENCES

1. Kieboom, A. P. G., and van Rantwijk, F., "Hydrogenation and Hydrogenolysis in Synthetic Organic Chemistry." Delft Univ. Press, Delft, 1977.
2. Stanislaus, A., and Cooper, B. H., *Catal. Rev. Sci. Eng.* **36**, 75 (1994).
3. Rylander, P. N., "Hydrogenation Methods." Academic Press, London, 1985.
4. Červený, L., and Růžička, V., *Catal Rev. Sci. Eng.* **24**, 503 (1982).
5. Augustine, R. L., "Catalytic Hydrogenation." Dekker, New York, 1975.
6. Rylander, P. N., "Catalytic Hydrogenation in Organic Syntheses." Academic Press, London, 1979.
7. Freifelder, M., "Catalytic Hydrogenation in Organic Synthesis, Procedures and Commentary." Wiley, New York, 1978.
8. "Catalytic Hydrogenation" (L. Červený, Ed.), Stud. Surf. Sci. Catal., Vol. 27. Elsevier, Amsterdam, 1986.
9. Siegel, S., *Adv. Catal.* **16**, 123 (1966).
10. Rader, Ch. P., and Smith, H. A., *J. Am. Chem. Soc.* **84**, 1443 (1962).
11. Hartog, F., and Zwietering, P., *J. Catal.* **2**, 79 (1963).
12. Bond, G. C., "Catalysis by Metals." Academic Press, London, 1962.
13. Wauquier, B., and Jungers, J. C., *Bull. Soc. Chim. France* 1280 (1957).
14. Burwell, R. L., Jr., *Chem. Rev.* **57**, 895 (1957).
15. Leitz, G., and Völter, J., *in* "Mechanism of Hydrocarbon Reactions." p. 151. Elsevier, Amsterdam, 1975.
16. Dufresne, P., Bigeard, P. H., and Billon, A., *Catal. Today* **1**, 367 (1987).
17. Armendia, N. A., Borau, V., Jimenez, C., and Marinas, J. M., *Bull. Soc. Chim. Belg.* **91**, 7743 (1982).
18. Gomez, R., Del Angelo, G., and Corro, G., *Nouv. Chem.* **4**, 219 (1980).
19. Vinnegra, M., Cordoba, G., and Gomez, R., *J. Mol. Catal.* **58**, 107 (1990).
20. Völter, J., *J. Catal.* **3**, 297 (1964).
21. Völter, J., Hermann, M., and Heise, K., *J. Catal.* **12**, 307 (1968).
22. Rahaman, M. V., and Vannice, M. A., *J. Catal.* **127**, 251, 267 (1991).
23. Keane, M. A., and Patterson, P. M., *J. Chem. Soc. Faraday Trans.* **92**, 1413 (1996).
24. Coughlan, B., and Keane, M. A., *Zeolites* **11**, 12 (1991).
25. Coughlan, B., and Keane, M. A., *Catal. Lett.* **5**, 101 (1990).
26. Keane, M. A., *Ind. J. Technol.* **30**, 51 (1992).
27. Keane, M. A., and Webb, G., *J. Catal.* **136**, 1 (1992).
28. Keane, M. A., *Can. J. Chem.* **72**, 372 (1994).
29. Smith, J. S., Thrower, P. A., and Vannice, M. A., *J. Catal.* **68**, 270 (1981).
30. Coenen, J. W. E., *Appl. Catal.* **75**, 193 (1991).
31. Greenfield, H., *Ann. N.Y. Acad. Sci.* **214**, 233 (1973).
32. Minot, C., and Gallezot, P., *J. Catal.* **123**, 341 (1990).
33. Candy, J., and Foilloux, P., *J. Catal.* **38**, 110 (1975).
34. Renouprez, A. J., and Clagnet, G., *J. Catal.* **74**, 296 (1982).
35. Dean, J. A., "Handbook of Organic Chemistry." McGraw–Hill, New York, 1987.
36. Martin, G. A., *J. Catal.* **60**, 345 (1979).
37. Frennet, A., Lienard, G., Crucq, A., and Degols, L., *J. Catal.* **53**, 150 (1978).
38. Ashmore, P. G., "Catalysis and Inhibition of Chemical Reactions." Butterworths, London, 1963.
39. Adamson, A. W., "Physical Chemistry of Surfaces," 5th ed. Wiley, New York, 1990.
40. Abon, M., Bertolini, J. C., Bily, J., Massardier, J., and Tardy, B., *Surf. Sci.* **162**, 395 (1985).
41. Tsai, M. C., and Muetterties, E. L., *J. Am. Chem. Soc.* **104**, 2543 (1992).
42. Galwey, A. K., *Adv. Catal.* **26**, 247 (1977).
43. Galwey, A. K., and Brown, M. E., *J. Catal.* **60**, 335 (1979).
44. Agrawal, R. K., *J. Thermal Anal.* **31**, 73 (1986); **35**, 73 (1989).
45. Exner, O., *Collect. Czech. Commun.* **38**, 1425 (1973).
46. Bartok, M., Czombos, J., Felfoldi, K., Gera, L., Gondos, Gy., Molmar, A., Northeisz, F., Palinko, I., Wittmann, Gy., and Zsigmond, A. G., "Stereochemistry of Heterogeneous Metal Catalysis." Wiley, New York, 1985.
47. Siegal, S., Smith, G. V., Dmuchovsky, B., Dubell, D., and Halpern, W., *J. Am. Chem. Soc.* **84**, 3136 (1962).
48. Kalsi, P. S., "Stereochemistry, Conformation and Mechanism." Wiley Eastern Ltd., New Delhi, 1990.
49. Snagovskii, Yu., Lyubarskii, G. D., and Ostrovskii, G. M., *Kinet. Katal.* **7**, 232 (1966).
50. van Meerten, R. Z. C., and Coenen, J. W. E., *J. Catal.* **46**, 13 (1977).
51. Prasad, K. H. V., Prasad, K. B. S., Muallikarjunan, M. M., and Vaidyeswaren, R., *J. Catal.* **84**, 65 (1983).
52. Zrnčević, S., and Rušić, D., *Chem. Sci. Eng.* **43**, 763 (1988).
53. Coughlan, B., and Keane, M. A., *J. Chem. Soc. Faraday Trans.* **86**, 3961 (1990).
54. Barbier, J., Morales, A., and Maurel, R., *Nouv. J. Chim.* **4**, 223 (1980).
55. Quinn, H. A., Graham, J. H., McKervey, M. A., and Rooney, J. J., *J. Catal.* **22**, 136 (1976).